Stripe domain coarsening in geographical small-world networks on a Euclidean lattice

R. Imayama and Y. Shiwa*
Statistical Mechanics Laboratory, Kyoto Institute of Technology, Matsugasaki, Sakyo-ku, Kyoto 606-8585, Japan
(Received 9 June 2009; published 22 September 2009)

We study phase ordering dynamics of spatially periodic striped patterns on the small-world network that is derived from a two-dimensional regular lattice with distance-dependent random connections. It is demonstrated numerically that addition of spatial disorder in the form of shortcuts makes the growth of domains much slower or even frozen at late times.

DOI: 10.1103/PhysRevE.80.036117 PACS number(s): 89.75.−k, 47.54.−r, 64.60.Cn, 05.65.+b

I. INTRODUCTION

Striped patterns abound in a variety of disparate systems, including Rayley-Bénard convection [1], microphase separation in block copolymers [2], magnetic solids and fluids (ferrofluids) [3], nonlinear optics in dissipative media [4], and ocular column formation [5]. They are sometimes called rolls, lamellar, or smectic patterns. Spirals and targets are the coherent structure that approximates quite well the striped pattern except for the existence of a point defect in the center, and these patterns are also prevalent in nature, most notably in physiological systems [6].

We investigate the formation of a stripe state. When a system is suddenly brought into an ordered phase where the initial state is thermodynamically unstable, the system develops a labyrinthine domain morphology consisting of locally ordered stripes of well-defined width. As time increases, stripes which are initially randomly oriented align in parallel, thereby creating an increasingly ordered pattern. Because of existence of the spatial period $(2\pi/k_0)$ of the ordered structure, the dynamics of this phase ordering (which is usually called domain coarsening) of striped states is quite intriguing in comparison with the much studied case of standard phase separation [7] for which $k_0=0$. Despite a great effort of research community, however, there are still conflicting results, and the explanations for different results are not completely consistent [8].

In theoretical models for the pattern formation, regular lattices are often taken to be the structure over which the phase ordering kinetics takes place, with the involving elements (molecules, neurons, etc.) interacting in a regular way. However, it has been found recently that the regular lattices are often inappropriate as the structure of interactions, which should instead be described by complex networks whose nodes represent the consisting elements and links representing the interactions among them [9–11]. Among the class of complex networks, a particular role is played by the small-world (SW) networks [12–14]. By introducing a certain amount of random connections into an initially regular network, it allows us to interpolate between the regular lattice and the random network. Outstanding topological properties of the SW networks are (i) a small average distance between nodes, which is a typical feature of random networks, and (ii) the degree of clustering, a measure of the local correlations among links of the network, has a high value as in regular lattices. For instance, neurobiological systems consisting of a large number of neurons possess such SW properties [15]. Particularly noteworthy in this connection is the observation of intercellular spiral waves in the hippocampus [16]. Furthermore, in the network model that mimics the regions of the brain where these spirals are observed, epileptic bursts and seizures occur only when the connectivity of the network is characterized as SW [17]. This observation, as a whole, suggests that spiral patterns in neuronal networks possibly arise from the SW topology.

Although pioneering numerical works have given some indications that the strong connectivity of SW enhances cooperative effects in, e.g., epidemic spreading [18] or synchronization [13,19], the relationship between the emergence of the SW regime and the arising of collective behaviors remains unclear [20–22].

Most of the studies done so far on complex networks have focused on topological networks where the nodes and links exist in some abstract space and the physical distance between nodes is irrelevant. However, in many real systems, the networks are embedded in spatial structure (Euclidean space) and possess geography in addition to their topology. For example, the neuronal networks in brains occupy three-dimensional space, and the likelihood of connections (hence interactions) between nodes is certainly affected by their geographical proximity. One thus expects that nontrivial consequences arise from the interplay between geography and topology [23]. From this perspective, the geographical effect on the topological properties of SW networks has been considered [24]. Also a good deal of study of the collective or dynamical processes on those SW networks has been reported. Examples of problems studied are the critical behavior of Ising model [25], diffusion [26,27], searching and navigation problems [28], epidemic spreading [29], and synchronization [30]. However, no agreement is yet reached on which structural property plays the most significant role in each case.

In this paper we study the domain coarsening of striped patterns in two-dimensional systems on square lattices which have the SW topology and in which interaction patterns depend on the Euclidean distance between nodes. We try to understand how the coarsening dynamics occurring on these networks depends on their geographical properties. To that end we use the simplest model that exhibits the phase ordering kinetics of lamellar patterns: the Swift-Hohenberg (SH)

*Corresponding author; shiway@kit.ac.jp

equation [31]. This is one of the most popular paradigmatic models that are employed to give a qualitatively correct description of the formation and evolution of lamellas observed in laboratory experiments [32]. However, so far there has been no attempt based on this prototypical model at showing the role of the geographic topology in the ordering dynamics. We study the coarsening in numerical simulations of this equation. The aforementioned connection to neuronal phenomena is expected to make our study of special relevance, and the results given below may furnish useful hints for understanding properties of collective neuronal behavior.

The paper is organized as follows. In Sec. II we briefly describe the SH model and define the geographical SW networks on which the ordering process occurs. Section III contains theoretical considerations to envisage the qualitative features of configurations during coarsening before studying numerically the growth of stripes in quantitative detail (Sec. IV). In Sec. V, a summary and discussion is given.

II. MODEL ON GEOGRAPHICAL SMALL-WORLD NETWORKS

To study the effect of the distance-dependent connectivity, we consider a class of networks, called hereafter geographical small-world (GSW) networks. To construct these networks, we start with a two-dimensional square lattice. We then add with a distance-dependent probability one shortcut per each bond (also called edge or link) on the original regular lattice, where the probability of a randomly chosen pair of vertices (nodes, sites) i and j being connected is given by $pf_\alpha(r_{ij})$, where [33]

$$f_\alpha(r) = [1 - \exp(-r^{-\alpha})]/\mathcal{N}. \tag{1}$$

Here r_{ij} is the Euclidean distance between the two vertices in the original lattice and $\mathcal{N}$ is the normalization factor; $\Sigma_j f_\alpha(r_{ij}) = 1$. The parameter p is thus defined as the probability per edge on the underlying lattice of there being a shortcut anywhere in the network. We do not remove any bonds from the regular lattice, and more than one bond between any two vertices as well as any bond connecting a vertex to itself is prohibited, so that an average coordination number z is given by $z=4(1+p)$. The case $\alpha=0$ is thus equivalent to the original SW network in Ref. [14], and we henceforth refer to this case as the plain SW network. Notice that

$$f_\alpha(r) \sim r^{-\alpha} \quad \text{as} \quad r \to \infty.$$

Accordingly the parameter α represents the strength of the distance-dependent suppression of the random long-range links and is sometimes called clustering exponent. In this way we obtain a two-parameter family of networks by tuning the values of p and α.

On this GSW network, evolution of the order parameter ψ_i, to be defined at each site i on the network, is described by the SH model,

$$\frac{\partial \psi_i}{\partial t} = \epsilon\psi_i - g\psi_i^3 - (\nabla^2 + k_0^2)^2\psi_i + \eta_i. \tag{2}$$

Here η_i is the delta-correlated Gaussian white noise. The positive constants g and k_0 are phenomenological parameters. The ϵ is the bifurcation parameter, with the transition to lamellar structures of spatial period of order k_0^{-1} appearing for $\epsilon > 0$ when $p=0$. The Laplacian operator in the present case consists of two terms,

$$\nabla^2 = (\nabla^2)^{nn} + (\nabla^2)^{sc}, \tag{3}$$

where $(\nabla^2)^{nn}$ is the Laplacian on the original square lattice, while $(\nabla^2)^{sc}$ is the one on the random part of the network. Both of these Laplacians are fully characterized by the adjacency matrix $\{A_{ij}\}$, taking the value $A_{ij}=1$ if the vertices at i and j are connected by an edge, whereas $A_{ij}=0$ otherwise. Thus, for example, for any quantity X_i on the site i of the network,

$$(\nabla^2)^{sc} X_i = \sum_j D_{ij} X_j, \tag{4}$$

with

$$D_{ij} \equiv A_{ij} - K_i \delta_{ij}. \tag{5}$$

The K_i is the degree of the vertex i counting the random links attached to this vertex: $K_i = \Sigma_j A_{ij}$.

III. PRELIMINARY CONSIDERATIONS

Before discussing numerical simulations in quantitative detail, it is worthwhile to have an approximate idea of qualitative features of the configurations that are expected to the model [Eq. (2)]. To that end, we will make a mean-field-type approximation to replace disorder with its average value. Thus we replace the diffusion operator ∇^2 in Eq. (2) with its average over random links,

$$[\nabla^2] = (\nabla^2)^{nn} + [(\nabla^2)^{sc}], \tag{6}$$

where

$$[(\nabla^2)^{sc}] X_i = \sum_j [D_{ij}] X_j,$$

$$[D_{ij}] = 4pf_\alpha(r_{ij}) - 4p\delta_{ij}. \tag{7}$$

In the above, $[\cdots]$ represents the average over the random links. With $\psi(\boldsymbol{r}) \equiv \psi_i$ ($\boldsymbol{r}$ being the position vector of the site i) and $\nabla^2 \equiv (\nabla^2)^{nn}$ for simplicity, Eq. (2) is then reduced to

$$\frac{\partial \psi(\boldsymbol{r})}{\partial t} = \epsilon\psi(\boldsymbol{r}) - g\psi^3(\boldsymbol{r}) - (\nabla^2 + k_0^2 - 4p)^2\psi(\boldsymbol{r}) - 8p(\nabla^2 + k_0^2 - 4p)\sum_{\boldsymbol{r}'} f_\alpha(|\boldsymbol{r} - \boldsymbol{r}'|)\psi(\boldsymbol{r}') - 16p^2 \sum_{\boldsymbol{r}'} \sum_{\boldsymbol{r}''} f_\alpha(|\boldsymbol{r} - \boldsymbol{r}'|) f_\alpha(|\boldsymbol{r}' - \boldsymbol{r}''|)\psi(\boldsymbol{r}''). \tag{8}$$

In the present analysis we wish to concentrate ourselves solely on the effect of random links, so that we employ further the Gaussian decomposition approximation [34] for the nonlinear term to replace

$$\psi^3 \to 3\langle\psi^2\rangle\psi,$$

where $\langle\psi^2\rangle$ is taken to be the steady-state average. Equation (8) now takes the form, in Fourier space,

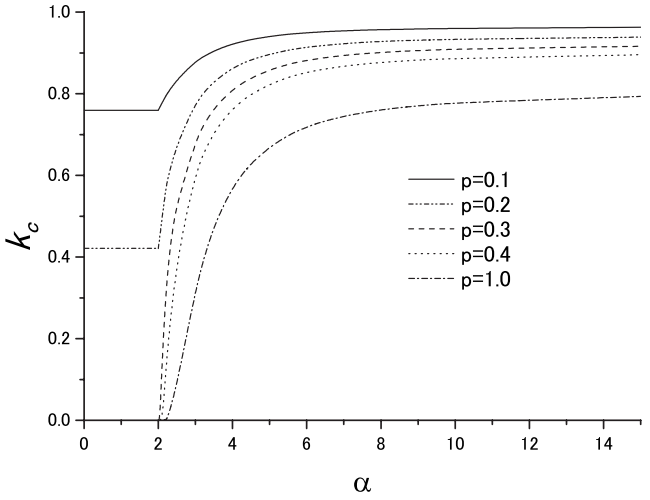

FIG. 1. Peak position k_c of the structure factor as a function of the clustering exponent α of the GSW network. The parameter k_0 used in this plot is $k_0=0.988$ (see Sec. IV A).

$$\partial_t \hat{\psi}(\boldsymbol{k}) = \{\tilde{\epsilon} + [k^2 - k_0^2 - 4pF_\alpha(k)]^2\}\hat{\psi}(\boldsymbol{k}), \tag{9}$$

where $\hat{\psi}(\boldsymbol{k})$ is the Fourier transform of $\psi(\boldsymbol{r})$ and $\tilde{\epsilon} \equiv 3g\langle\psi^2\rangle - \epsilon$ is the renormalized control parameter, which is assumed to be positive. Also

$$F_\alpha(k) = \frac{\int_0^\infty drrf_\alpha(r)[J_0(kr) - 1]}{\int_0^\infty drrf_\alpha(r)}, \tag{10}$$

where $J_0(z)$ is the Bessel function of the first kind. We here remind readers again that the calculation is being done in two spatial dimensions.

The linearized form [Eq. (9)] then enables one to calculate the structure factor $S(k)$ defined by $S(k)=\langle|\hat{\psi}(\boldsymbol{k})|^2\rangle$. Consequently, the peak position k_c of $S(k)$ is determined as the root of the equation

$$k^2 - k_0^2 - 4pF_\alpha(k) = 0. \tag{11}$$

Since $F_\alpha(k)=-1$ for $\alpha \leq 2$, we immediately find that

$$k_c = \begin{cases} \sqrt{k_0^2 - 4p} & \text{if } p < k_0^2/4 \\ 0 & \text{otherwise.} \end{cases} \tag{12}$$

For $\alpha > 2$, Eq. (11) is solved numerically and the obtained k_c is exhibited in Fig. 1 as a function of α for varying values of p.

From the above results we first note that for $p < k_0^2/4$, we always have a stripe state irrespective of the value of α. Particularly in this case, if $\alpha \leq 2$, the wave number of the striped pattern is equal to the plain SW value [35]. On the other hand, for $p \geq k_0^2/4$, the transition from the homogeneous to the stripe state occurs as α crosses the threshold value $\alpha_c \approx 2$ from below. Moreover, we find that decreasing the range of random links (i.e., increasing α) pushes the spatial period to lower values. All these qualitative features are confirmed by numerical simulations of Eq. (2), to which we now turn in Sec. IV.

IV. SIMULATION RESULTS

A. Methodology

We shall consider now the phase ordering of the present system for different choices of the shortcut parameter p and the clustering exponent α. We have carried out simulations based on Eq. (2). Throughout this section we consider only the case $\eta_i=0$. A two-dimensional space is divided into square cells with periodic boundary conditions. The cell size is set to be unity. Unless otherwise stated, all demonstrations in this paper are results obtained on a system of 1024×1024 lattice. In order to allow easier exploration of the long-time regime of pattern formation, we follow the spirit of the cell-dynamical-system (CDS) method [36]. For Eq. (2) we solved the following CDS model:

$$\psi(n,t+1) = A \tanh \psi(n,t) - L(\nabla^2 + \kappa)^2 \psi(n,t), \tag{13}$$

where $\psi(n,t)$ is the order parameter associated with a lattice site labeled by n at time t. The Laplacian is evaluated as given in Eq. (3). Initial conditions for $\psi(n)$ were the spatially random distribution between ± 0.01. The parameters used were $A=1.0015$, $L=0.0087$, and $\kappa=0.9$. The choice of these parameters is dictated by a linear stability analysis of the discrete map [Eq. (13)]. In the absence of shortcuts, the homogeneous state ($\psi=0$) is destabilized for $A>1$, and the wave number k_0 of the most unstable mode is given by

$$k_0 = \arccos\left(\frac{2-\kappa}{2}\right). \tag{14}$$

Thus with $\kappa=0.9$, we have $k_0=0.988$ and the aspect ratio Γ as defined by the ratio of the system size to $2\pi/k_0$ is $\Gamma \approx 160$. Hence the finite-size effects are assumed to be negligible in the gross behavior of coarsening, and one sample of size 1024^2 is sufficient for our purpose.

We have constructed the GSW network as defined in Sec. II. The topological characteristics of our networks with and without geographical organization are compared in Fig. 2. Since the frequently used clustering coefficient, C_3, as computed via the number of triangles in the network is generically zero for the plain SW graph on the square lattice [37], it is unable to quantify the high clustering actually present in our network structure. (A triangle is a set of three vertices with edges between each pair of vertices.) Therefore we have measured the grid coefficient C_4 [38] that is defined as the relative abundance of the quadrilaterals in the network and take the sum $C_{34} \equiv C_3 + C_4$ as a measure of the clustering in our GSW networks. The average shortest-path length ℓ was measured using a burning algorithm, also called breadth-first search [39]. Figure 2 clearly demonstrates that the network has the SW property in some regions of its parameter space $\{p, \alpha\}$.

B. Results

1. Trends with parameters

Figure 3 shows the morphology of patterns observed during the coarsening process after the same initial conditions for different α and p. As α is increased, the stripes become

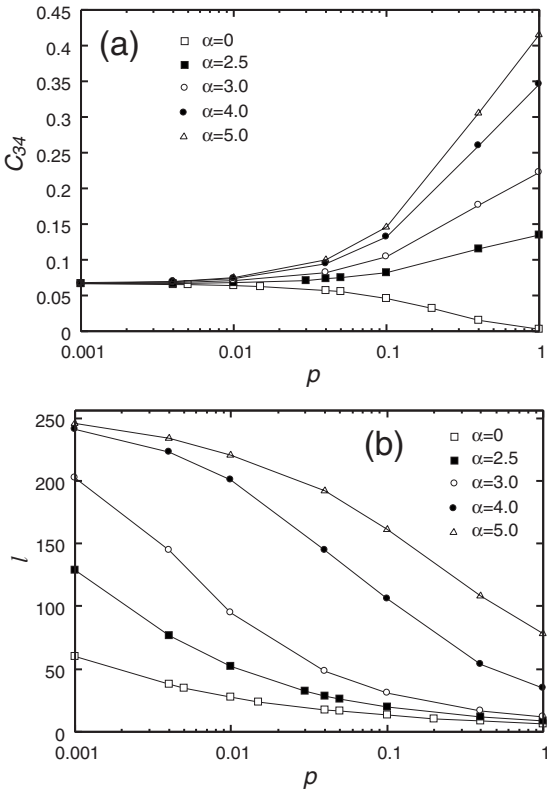

FIG. 2. (a) The clustering coefficient C_{34} and (b) the average shortest-path length ℓ as a function of p for different α. Each data point is obtained with the 512^2 lattice system.

more ordered [panel (a)], indicating the coarsening is enhanced. In cases where the pattern freezes into an inhomogeneous state for $\alpha=0$, the frozen state disappears as α is increased [panel (b)]. Further increase in α results again in the enhancement. It is also apparent when we look at panel (c) that there is a general trend of the GSW topology promoting an increase in the stripe wave number with increasing value α.

Quantitative trend of the variation in the coarsening dynamics with the value of α is shown in Fig. 4. Here we computed the circularly averaged structure factor $S(k,t)$ defined by

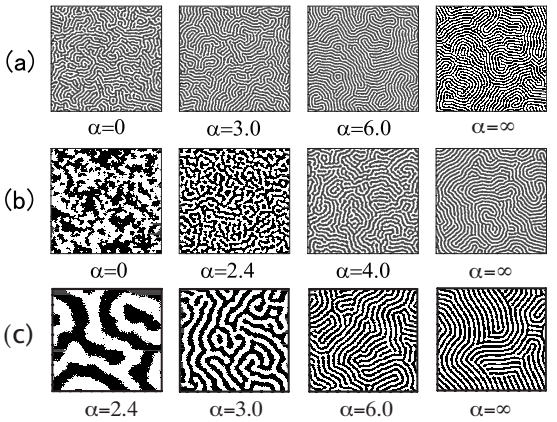

FIG. 3. Patterns achieved after 398 107 time steps from the same initial conditions for various values of α at (a) $p=0.1$, (b) $p=0.4$, and (c) $p=1.0$. The white regions denote positive values of the order parameter ψ, while the gray ones denote negative ψ. Each figure exhibits a central 256^2 portion of the 1024^2 lattice system.

$$S(k,t) = \langle \hat{\psi}(\mathbf{k},t)\hat{\psi}^*(\mathbf{k},t)\rangle, \tag{15}$$

where $\hat{\psi}(\mathbf{k},t)$ is the Fourier transform of the order parameter ψ at time t and the orientation of the wave vector $\mathbf{k}$ is averaged over. To remove any effect due to the finiteness of the ratio of the thickness of domain walls to the domain size, we calculated $S(k,t)$ after the data were hardened using the transformation $\psi \to \mathrm{sgn}\ \psi$. Also shown in Fig. 4 is the orientational field correlation function, $C_2(r,t)$. It is defined by

$$C_2(|\mathbf{r}-\mathbf{r}'|,t) = \langle \exp[i2\{\theta(\mathbf{r},t) - \theta(\mathbf{r}',t)\}]\rangle, \tag{16}$$

averaging over the spatial coordinates $\mathbf{r}$ and $\mathbf{r}'$ for fixed $|\mathbf{r}-\mathbf{r}'|$ for each time t. Here the local orientation $\theta(\mathbf{r},t)$ of the stripe is defined as the angle in the direction normal to the stripe axis, and it was computed with a slight modification [40] of the wavelet transform method in Ref. [41]. The factor of 2 is required by a twofold symmetry of striped patterns.

It is seen in Fig. 4(a) that there is a shift in the position where $S(k)$ has its maximum, the shift occurring toward larger k with increasing α. Accompanied with it are narrowing of the scattering profile and the attendant increase in the peak intensity. Figure 4(b) shows that the orientational cor-

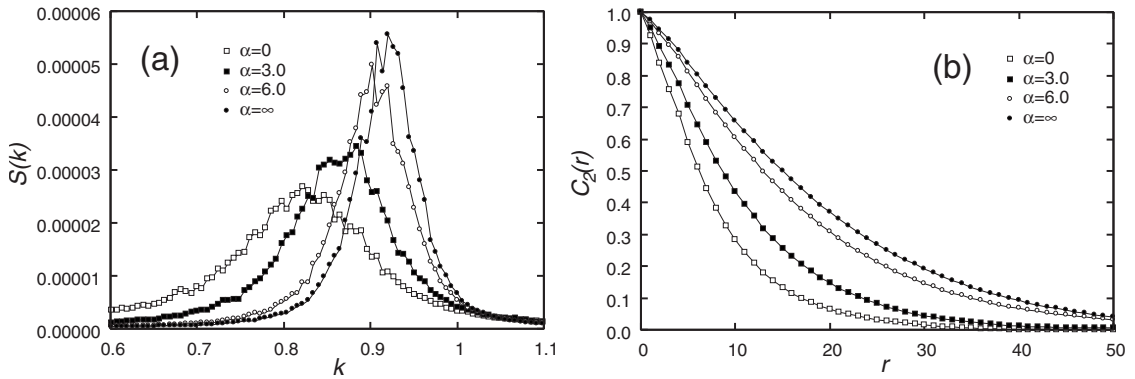

FIG. 4. (a) The circularly averaged structure factor $S(k)$ and (b) the orientational correlation function $C_2(r)$ at time step 398 107 for various values of α with $p=0.1$. The $S(k)$ is in arbitrary units.

relation function $C_2(r)$ is a monotonically decreasing function, and it is clear that there is a dependence on the value of α.

The peak position (k_c) of the structure factor $S(k)$ represents the width of stripes, and the full width at half maximum, δk, defines the characteristic length scale of the striped domain by $\xi=2\pi/\delta k$. We extracted k_c and δk from a squared Lorentzian fit to $S(k)$ at each time t,

$$S(k) = a^2/[(k^2-b)^2+c^2]^2. \tag{17}$$

The length scale $\xi(t)$ measured in this way is well fitted by a power law $\xi(t)\sim t^{\beta}$ at the late stage of coarsening. The peak position k_c and the growth exponent β are plotted as a function of α in Fig. 5 for various p. Comparing with Fig. 1 shows that the predicted effects on k_c of the geographic parameter α are much stronger than those observed in simulations. (As is usual with critical phenomena, transitions near $\alpha\approx 2$ are smeared due to the finite-size effects.) Evidently, to obtain a more quantitative agreement would require the higher-order corrections in the disorder-average perturbation theory [27,42] in which the mean-field prediction appears as the lowest-order term. It is, however, not within the scope of the present paper and we leave it an open question.

As an alternative measure of the domain growth, we have also extracted the orientational correlation length, ξ_o, from the decay of $C_2(r)$ as the value of r at which $C_2(r)$ reaches the value 0.3; with the other values chosen we found that it entailed little changes in the growth exponent. The $\xi_o(t)$ thus obtained is found to obey the power law growth again but with a growth exponent different from β. The latter result can be understood if one notes that in the spatially periodic patterns as observed in the present study, the length scale extracted from $S(k,t)$ is a complicated convolution of the domain size and the variation in the local wave number k, and it does not have the same geometrical interpretation as the length scale extracted from $C_2(k,t)$ [43]. However, we have found that the two different measures of coarsening exhibit the similar trends concerning their dependence on the parameters α and p.

Representative results of the behavior reported above are summarized in Table I, where we list the effects that different topologies have on the growth of striped domains. In the case of plain SW networks, the structure of networks is solely parametrized by p, which represents the degree of randomness present in the system; for $p=0$ the lattice is regular, while for $p=1$ it is fully random. Clearly we see that the regular lattice is an optimal architecture in terms of coarsening efficiency. The driving force for coarsening of striped patterns is greatly reduced due to disorders introduced by shortcuts which tend to pin the interfaces in order parameter configurations that are locally metastable [35]. Here we remind the reader that the competition between interactions on different length scales causes the emergence of a large number of metastable states, and this is generally considered as a condition for glassiness that is incurred in the system [44].

Now let us examine the GSW case. The second and the third columns of Table I imply that the limit $\alpha\to\infty$ or $p\to 0$ will perform fastest in domain growth. In fact we found that the regular lattice again performs faster than any other

TABLE I. Variation in main characteristics of the network and the pattern for a change in p or α for the plain and the geographical SW networks. On the change in p or α indicated in the second row, the network topology changes as indicated in the third row. The characteristics given are clustering coefficient C_4 or C_{34}, average shortest-path length ℓ, peak position of structure factor k_c, and domain growth exponent β.

Plain SW	Geographical SW	
$p\downarrow$	$\alpha\uparrow$ ($p\neq 0$ fixed)	$p\downarrow$ ($\alpha\neq 0$ fixed)
Random $\to$ Regular	Plain SW $\to$ Regular [a]	Random $\to$ Regular
$C_4\uparrow$	$C_{34}\uparrow$	$C_{34}\uparrow$ if $\alpha\lesssim 2$; $C_{34}\downarrow$ if $\alpha>2$
$\ell\uparrow$	$\ell\uparrow$	$\ell\uparrow$
$k_c\uparrow$	$k_c\uparrow$	$k_c\uparrow$
$\beta\uparrow$	$\beta\uparrow$	$\beta\uparrow$

[a]Note, however, that the limit $\alpha\to\infty$ does not always imply the regular lattice, as explained in the main text (Sec. IV B 1).

disordered networks, the exponent attaining the by-now-classical (albeit theoretical interpretation of this value is still missing at present [8]) value $\beta\simeq 1/5$. We remark in this connection that the GSW network is equivalent to a regular lattice either in the case $p=0$ or in the case $\alpha=\infty$ with $p=1$, while the case $\alpha=\infty$ with $p\neq 1$ corresponds to the disordered lattice (the reason being that in this case a bond which connects a vertex to its next-nearest neighbors on the undelying lattice is added at random with probability p).

2. Role of clustering in slow domain growth

We have shown above that the growth exponent β takes on the maximum value in the regular lattice. If one looks more closely at the results in Table I, one notices an apparently perplexing behavior of β regarding its dependence on the two topological characteristics (i.e., ℓ and $C\equiv C_4$ or C_{34}) of SW networks. On one hand, in the plain SW network C_4 increases as p approaches its regular-lattice value ($p=0$). On the other hand, in the GSW network C_{34} decreases as $p\to 0$ for $\alpha>2$. In both type of networks, however, ℓ increases with the approach to the regular lattice. We may thus ask whether a system can have the more enhanced coarsening with a higher C or with a lower.

What we are then plotting in Fig. 6 is the variation in the growth exponent with the strength of the clustering effect C_{34} when the average shortest-path length ℓ is kept fixed at a given value. (In this way we have singled out the role of C_{34} or ℓ in the coarsening dynamics.) Note that choosing either $\ell\approx 35$ or $\ell\approx 13$, we are now examining a region of the parameter space which presents the small-world property, i.e., a region in which clustering is high and mean node-node distance is simultaneously low (see Fig. 2). Clearly the exponent β is a decreasing function of C_{34} and the downward slope becomes flattened out at larger C_{34} for which we observed the pattern effectively gets stuck in the disordered stripe state. In order to understand this behavior, we made a histogram of the local clustering coefficients of vertices (the average of which over all the vertices is thus our clustering

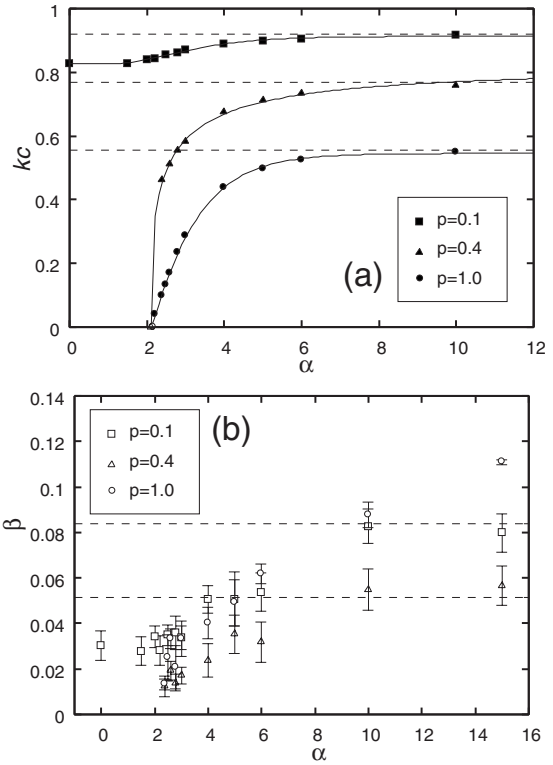

FIG. 5. (a) The peak position k_c of the structure factor at time step 398 107 and (b) the growth exponent β versus α for $p=0.1$, 0.4, and 1.0. The open symbols in (a) denote the extrapolated threshold values for $p=0.4$ and $p=1.0$, which are obtained by the nonlinear curve fit to the data points (filled symbols). The dashed lines in (a) represent the values at $\alpha=\infty$ for respective p's. The dashed lines in (b) indicate the values of β at $\alpha=\infty$ for $p=0.4$ (lower) and 0.1 (upper) and for $p=1.0$ we found $\beta=0.20$ at $\alpha=\infty$.

coefficient C_{34}). We found, when C_{34} increases, the distribution of the local clustering coefficients becomes very broadened. Physically this is because in the present case, if C_{34} increases, both α and p are simultaneously increased; thus not only the density of local connections is increased but an increasing number of network configurations become possible. This in turn allows the system to support a large number of metastable states, i.e., a necessary prerequisite to glassiness.

Also evident from the figure is that as a function of ℓ, the growth exponent β is an increasing function. As the leftmost end of each curve of data corresponds to the $\alpha=0$ case, the dashed line combining these ends represents the plain SW behavior of β as a function of both ℓ and C_4. With this dashed curve one can immediately understand why in Table I β appears as an increasing function of C_4 in the plain SW network, in marked contrast to the GSW case with $\alpha>2$.

V. SUMMARY AND DISCUSSION

We have presented a study of the SH model for the formation of striped patterns on the GSW network. In SW networks, the original local (short-range) interaction topology is extended to include possibly long-ranged links. Recall that the striped pattern results from the competing interactions:

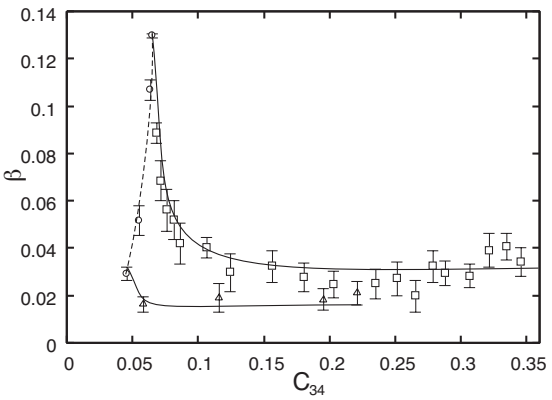

FIG. 6. Growth exponent β versus the clustering coefficient C_{34} when the average shortest-path length ℓ is fixed at $\ell\approx35$ (top) and $\ell\approx13$ (bottom). The data are computed averaging over five different realizations of the network of size 512^2. The solid lines are drawn as a guide for the eyes. The open circular symbols connected by the dashed curve represent the case of the plain SW networks; from top to bottom $\ell\approx35,27,16,13$.

one favors the homogenization, whereas the other wants the heterogeneous distribution of the order parameter field. Therefore the following question that we have pondered in the present paper is nontrivial: Could the long-range random connections present in the networks enhance the spatial stripe organization process? Or, will this rather spoil the organization process with its concomitant effect of partially destroying the spatial heterogeneity?

Our study has revealed that spatial disorder in the form of random shortcuts in the network always inhibits rather than facilitates the ordering dynamics of stripes, making the stripe ordering harder to achieve. This conclusion is irrespective of whether the SW network is plain or geographical in which the interaction is slowly decaying with Euclidean distance.

Having focused our attention to the general question above, we may now ask a more specific question: How long ranged are nonlocal connections when they become effective in freezing the coarsening process? That is, does there exist any typical distance between the ends of shortcut at which the crossover to very slow ordering dynamics occurs? To answer the question, let us construct from our GSW network a new network topology with pruned connections, which is akin to the so-called [13] uniform spatial graphs. We do this as follows: the random shortcuts whose spatial length is longer than the cutoff distance, ℓ_c, are all deleted from the GSW network.

Simulations were then performed on such networks with various values chosen for ℓ_c, otherwise the simulation method being same as described in Sec. IV A. Figure 7 shows the growth exponent thus obtained as a function of ℓ_c, in which the dimensionless variable ℓ_c/λ is used where λ is a spatial period of the striped pattern that is observed for a respective data point. We see that in the case a frozen stripe state is eventually reached ($p=0.3$), the exponent decreases rapidly in a rather small region of ℓ_c/λ near $\ell_c/\lambda\approx1/2$. This suggests that not too long shortcuts of a distance comparable to the stripe width suffice for the freezing to be induced. Similar observation was made in our previous study of coars-

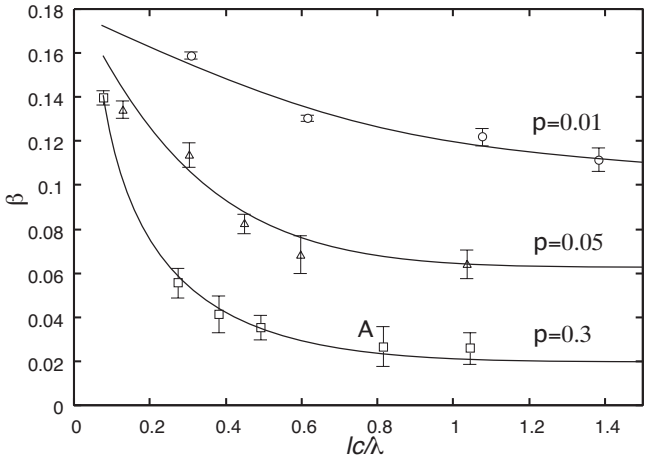

FIG. 7. Growth exponent β versus ℓ_c/λ for various p at $\alpha=3.6$. Five samples of size 512^2 are used to obtain each data. The growth exponents in this figure are measured on the geographical SW networks in which every shortcut whose Euclidean length is longer than ℓ_c is deleted. The λ is calculated with $\lambda=2\pi/k_c$, k_c being the peak position of $S(k)$ at time step 398 107. A sample configuration which corresponds to point A is shown in Fig. 8.

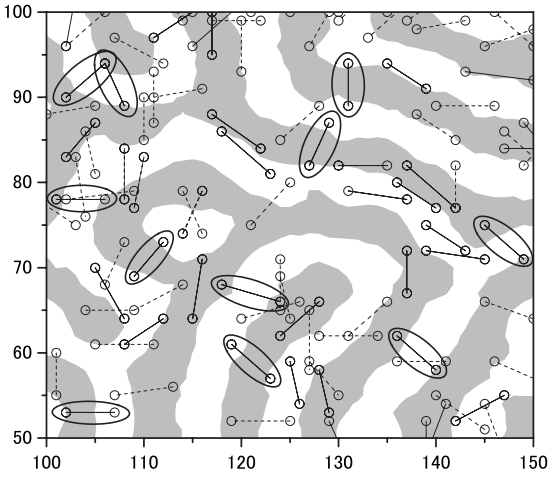

FIG. 8. Glassy configuration for $\ell_c/\lambda \approx 0.8$ ($\ell_c=7$) in the presence of unfavorable shortcuts (encircled with ellipse) which tend to pin the stripe interfaces. A solid line represents the shortcut connecting the like nodes, while a dashed line contains an unlike pair. For clarity only the shortcuts whose Euclidean length is five or more are drawn. Shown here is a 50^2 portion of the 512^2 lattice system.

ening dynamics on the plain SW networks [45]. These findings are also in accord with the proposed scenario [46] for a glassy state in general that in a system with competing interactions relevant to the formation of stripes, emergence of glassiness is tied to the critical value of a characteristic length scale which is close to the stripe width.

The emergence of dynamically frozen configurations can be interpreted qualitatively by the following argument. Consider Fig. 8 which shows a typical frozen pattern that was observed in our simulations conducted at parameters corresponding to point A in Fig. 7. The shortcut that connects two nodes of the same sign of ψ (or "like" pairs [21]) is represented by a solid line. Among these shortcuts, those encircled by ellipse (referred to as "unfavorable" shortcuts) connect like nodes both contained in the disparate and, say, white regions. When the shortcut length (ℓ_s) is smaller than the typical distance ($\lambda/2$) between stripes, stripe domain coarsening is slowed down by like pairs since "unlike" pairs turn more easily to like pairs than the contrary. In this case, however, the presence of like pairs is not so effective as to arrest striped configurations as a whole. On the increase in ℓ_s to $\ell_s \approx \lambda/2$, on the other hand, unfavorable shortcuts can now be generated dynamically. Any distorted interface passing through the unfavorable shortcut cannot easily straighten or flatten out since it is energetically unfavorable. Thus the unfavorable shortcuts in this case play the role of pinning sites. For rather larger p, the system contains many unfavorable pinning sites as in Fig. 8, which in turn generate metastability that many different microscopic configurations are locally stable. Therefore the system is prevented from reaching a configuration with straight domain boundaries, leading to a very slow or arrested dynamics.

Target patterns as well as spiral patterns can be found in the heart and the brain [6,16]. In this case, the desire to understand how the functional disorders such as fibrillation and epilepsy are established and to develop treatment to avert the establishment of those abnormal organizations underlies much of the research on the spatial organization of cardiac and neuronal activities [6]. In view of the fact that SW topologies have been associated with those activity patterns [17,47], our results that increasing disorder (p) or the range of connection can destroy the lamellar structure, and particularly that the presence of relatively short-ranged shortcuts is responsible for freezing the coarsening process will certainly point toward intriguing possibility of the role of GSW connections in removal of the physiological abnormalitites.

To understand the role of randomness in ordering dynamics of striped patterns, we have confined ourselves to the small-world effects. In real network structures, however, there is another generic feature that is missing from the present study. These networks have a highly inhomogeneous structure reflected in their fat-tailed degree distribution $P(K)$ which follows a power law $P(K) \sim K^{-\gamma}$, thus being designated as scale-free networks [9–11]. Therefore it would be interesting to study how the coarsening dynamics changes in that case, and we plan to present such analysis elsewhere.

[1] Y. Hu, R. Ecke, and G. Ahlers, Phys. Rev. E **48**, 4399 (1993).
[2] C. Harrison, Z. Cheng, S. Sethuraman, D. A. Huse, P. M. Chaikin, D. A. Vega, J. M. Sebastian, R. A. Register, and D. H. Adamson, Phys. Rev. E **66**, 011706 (2002).
[3] M. Seul and R. Wolfe, Phys. Rev. A **46**, 7519 (1992).
[4] F. T. Arecchi, G. Giacomelli, P. L. Ramazza, and S. Residori, Phys. Rev. Lett. **67**, 3749 (1991).
[5] D. H. Hubel and T. N. Wiesel, Proc. R. Soc. London, Ser. B **198**, 1 (1977).
[6] L. Glass and M. C. Mackey, *From Clocks and Chaos* (Princeton University Press, Princeton, 1988).
[7] A. J. Bray, Adv. Phys. **43**, 357 (1994).
[8] Y. Shiwa, in *Statistical and Condensed Matter Physics: Over the Horizon*, edited by S. Fujita *et al.* (Nova Science, New York, 2007), Chap. 1.
[9] R. Albert and A.-I. Barabási, Rev. Mod. Phys. **74**, 47 (2002).
[10] S. N. Dorogovtsev and J. F. F. Mendes, Adv. Phys. **51**, 1079 (2002); *Evolution of Networks* (Oxford University Press, Oxford, 2003).
[11] M. E. J. Newman, SIAM Rev. **45**, 167 (2003).
[12] D. J. Watts and S. H. Strogatz, Nature (London) **393**, 440 (1998).
[13] D. J. Watts, *Small Worlds: The Dynamics of Networks between Order and Randomness* (Princeton University Press, Princeton, 1999).
[14] M. E. J. Newman and D. J. Watts, Phys. Rev. E **60**, 7332 (1999).
[15] O. Shefi, I. Golding, R. Segev, E. Ben-Jacob, and A. Ayali, Phys. Rev. E **66**, 021905 (2002).
[16] M. E. Harris-White, S. A. Zanotti, S. A. Frautschy, and A. C. Charles, J. Neurophysiol. **79**, 1045 (1998).
[17] T. I. Netoff, R. Clewley, S. Arno, T. Keck, and J. A. White, J. Neurosci. **24**, 8075 (2004).
[18] D. H. Zanette, Phys. Rev. E **64**, 050901(R) (2001); O. Miramontes and B. Luque, Physica D **168–169**, 379 (2002).
[19] L. F. Lago-Fernández, R. Huerta, F. Corbacho, and J. A. Sigüenza, Phys. Rev. Lett. **84**, 2758 (2000); P. M. Gade and C.-K. Hu, Phys. Rev. E **62**, 6409 (2000); H. Hong, M. Y. Choi, and B. J. Kim, *ibid.* **65**, 026139 (2002); M. Barahona and L. M. Pecora, Phys. Rev. Lett. **89**, 054101 (2002).
[20] X. Guardiola, A. Díaz-Guilera, M. Llas, and C. J. Pérez, Phys. Rev. E **62**, 5565 (2000); T. Nishikawa, A. E. Motter, Y.-C. Lai, and F. C. Hoppensteadt, Phys. Rev. Lett. **91**, 014101 (2003); H. Hong, B. J. Kim, M. Y. Choi, and H. Park, Phys. Rev. E **69**, 067105 (2004).
[21] D. Boyer and O. Miramontes, Phys. Rev. E **67**, 035102(R) (2003).
[22] S. Boccaletti, V. Latora, Y. Moreno, M. Chavez, and D.-U. Hwang, Phys. Rep. **424**, 175 (2006).
[23] M. T. Gastner and M. E. J. Newman, Eur. Phys. J. B **49**, 247 (2006).
[24] M. Kuperman and G. Abramson, Phys. Rev. E **64**, 047103 (2001); P. Sen and B. K. Chakrabarti, J. Phys. A **34**, 7749 (2001); C. F. Moukarzel and M. Argollo de Menezes, Phys. Rev. E **65**, 056709 (2002); P. Sen, K. Banerjee, and T. Biswas, *ibid.* **66**, 037102 (2002); T. Petermann and Paolo De Los Rios, *ibid.* **73**, 026114 (2006).
[25] A. Chatterjee and P. Sen, Phys. Rev. E **74**, 036109 (2006); Y-F. Chang, L. Sun, and X. Cai, *ibid.* **76**, 021101 (2007); M. Woloszyn, D. Stauffer, and K. Kulakowski, Eur. Phys. J. B **57**, 331 (2007).
[26] S. Jespersen and A. Blumen, Phys. Rev. E **62**, 6270 (2000).
[27] B. Kozma, M. B. Hastings, and G. Korniss, Phys. Rev. Lett. **95**, 018701 (2005); J. Stat. Mech.: Theory Exp. **2007**, P08014.
[28] J. Kleinberg, Nature (London) **406**, 845 (2000); Proceedings of the 32nd ACM Symposium on Theory of Computing, 2000 (unpublished), p. 163; Z.-G. Huang, S.-J. Wang, X.-J. Xu, and Y.-H. Wang, EPL **81**, 28001 (2008); C. Cartozo and Paolo De Los Rios, e-print arXiv:0901.4710.
[29] W.-P. Guo, X. Li, and X.-F. Wang, Physica A **380**, 684 (2007); F. Linder, J. Tran-Gia, S. R. Dahmen, and H. Hinrichsen, J. Phys. A **41**, 185005 (2008).
[30] C.-Y. Yin, B.-H. Wang, W.-X. Wang, and G.-R. Chen, Phys. Rev. E **77**, 027102 (2008).
[31] J. Swift and P. C. Hohenberg, Phys. Rev. A **15**, 319 (1977); P. C. Hohenberg and J. B. Swift, *ibid.* **46**, 4773 (1992).
[32] M. C. Cross and P. C. Hohenberg, Rev. Mod. Phys. **65**, 851 (1993).
[33] M. Biskup, Ann. Probab. **32**, 2938 (2004).
[34] See, for instance, G. H. Fredrickson and K. Binder, J. Chem. Phys. **91**, 7265 (1989).
[35] R. Imayama and Y. Shiwa, Physica A **387**, 1033 (2008).
[36] Y. Oono and S. Puri, Phys. Rev. Lett. **58**, 836 (1987); Y. Oono and Y. Shiwa, Mod. Phys. Lett. B **1**, 49 (1987).
[37] M. E. J. Newman, Comput. Phys. Commun. **147**, 40 (2002).
[38] G. Caldarelli, R. Pastor-Satorras, and A. Vespignani, Eur. Phys. J. B **38**, 183 (2004).
[39] M. E. J. Newman, Phys. Rev. E **64**, 016132 (2001).
[40] Y. Yokojima and Y. Shiwa, Phys. Rev. E **65**, 056308 (2002).
[41] M. C. Cross, D. Meiron, and Y. Tu, Chaos **4**, 607 (1994).
[42] B. Kozma, M. B. Hastings, and G. Korniss, Phys. Rev. Lett. **92**, 108701 (2004).
[43] J. J. Christensen and A. J. Bray, Phys. Rev. E **58**, 5364 (1998).
[44] T. R. Kirkpatrick and D. Thirumalai, Phys. Rev. Lett. **58**, 2091 (1987); J. Schmalian and P. G. Wolynes, *ibid.* **85**, 836 (2000).
[45] R. Imayama and Y. Shiwa, *Complex Systems*, AIP Conf. Proc. No. 982 (AIP, New York, 2008), p. 403.
[46] H. Westfahl, J. Schmalian, and P. G. Wolynes, Phys. Rev. B **64**, 174203 (2001); M. Tarzia and A. Coniglio, Phys. Rev. Lett. **96**, 075702 (2006).
[47] A. Roxin, H. Riecke, and S. A. Solla, Phys. Rev. Lett. **92**, 198101 (2004).